



OPEN ACCESS

EDITED BY

Juan Carlos Gallardo-Pérez,
National Institute of Cardiology Ignacio
Chavez, Mexico

REVIEWED BY

Adnin Ashrafi,
Retina Foundation of the Southwest,
United States
Erika Monserrat Navarro Araujo,
National Autonomous University of Mexico,
Mexico

*CORRESPONDENCE

Zhu Chen
✉ chenzhu510@126.com

RECEIVED 14 January 2024

ACCEPTED 14 June 2024

PUBLISHED 27 June 2024

CITATION

Deng H, Wang Z, Zhu C and Chen Z (2024)
Prolyl hydroxylase domain enzyme PHD2
inhibits proliferation and metabolism in
non-small cell lung cancer cells in HIF-
dependent and HIF-independent manners.
Front. Oncol. 14:1370393.
doi: 10.3389/fonc.2024.1370393

COPYRIGHT

© 2024 Deng, Wang, Zhu and Chen. This is an
open-access article distributed under the terms
of the [Creative Commons Attribution License
\(CC BY\)](https://creativecommons.org/licenses/by/4.0/). The use, distribution or reproduction
in other forums is permitted, provided the
original author(s) and the copyright owner(s)
are credited and that the original publication
in this journal is cited, in accordance with
accepted academic practice. No use,
distribution or reproduction is permitted
which does not comply with these terms.

Prolyl hydroxylase domain enzyme PHD2 inhibits proliferation and metabolism in non-small cell lung cancer cells in HIF-dependent and HIF-independent manners

Hongyan Deng^{1,2}, Zixuan Wang¹,
Chunchun Zhu¹ and Zhu Chen^{3*}

¹Institute of Hydrobiology, Chinese Academy of Sciences, Wuhan, China, ²College of Life Science, Wuhan University, Wuhan, China, ³Department of Reproduction, Maternal and Child Health Hospital of Hubei Province, Tongji Medical College, Huazhong University of Science and Technology, Wuhan, China

Prolyl hydroxylase domain protein 2 (PHD2) is one of the intracellular oxygen sensors that mediates proteasomal degradation of hypoxia-inducible factor (HIF)- α via hydroxylation under normoxic conditions. Because of its canonical function in the hypoxia signaling pathway, PHD2 is generally regarded as a tumor suppressor. However, the effects of PHD2 in tumorigenesis are not entirely dependent on HIF- α . Based on analysis of data from the Cancer Genome Atlas (TCGA) database, we observed that the expression of *PHD2* is upregulated in non-small cell lung cancer (NSCLC), which accounts for approximately 80–85% of lung cancers. This suggests that PHD2 may play an important role in NSCLC. However, the function of PHD2 in NSCLC remains largely unknown. In this study, we established *PHD2*-deficient H1299 cells and *PHD2*-knockdown A549 cells to investigate the function of PHD2 in NSCLC and found that PHD2 suppresses cell proliferation and metabolism but induces ROS levels in human NSCLC cells. Further results indicated that the function of PHD2 in NSCLC is dependent on its enzymatic activity and partially independent of HIF. Moreover, we performed RNA-sequencing and transcriptomic analysis to explore the underlying mechanisms and identified some potential targets and pathways regulated by PHD2, apart from the canonical HIF-mediated hypoxia signaling pathway. These results provide some clues to uncover novel roles of PHD2 in lung cancer progression.

KEYWORDS

PHD2, prolyl hydroxylase, non-small cell lung cancer, HIF-dependent, HIF-independent

1 Introduction

Prolyl hydroxylase domain protein 2 (*PHD2*, also known as egg-laying defective nine 1, *EGLN1*) belongs to the family of prolyl hydroxylase domain proteins (PHDs). The PHD family is an evolutionarily conserved superfamily of dioxygenases, consisting of four members: *PHD1* (*EGLN2*), *PHD2* (*EGLN1*), *PHD3* (*EGLN3*), and the less studied *PHD4* (*P4H-TM*, *EGLN4*) (1–5). The hydroxylation reaction catalyzed by PHDs is dependent on their conserved C-terminal catalytic domain, oxygen (O₂), ferrous iron (Fe²⁺), 2-oxoglutarate (2-OG), and ascorbic acid (vitamin C) (6). PHDs act as intracellular oxygen sensors that mediate the proteasomal degradation of hypoxia-inducible factor (HIF)- α via hydroxylation under normoxic conditions (7, 8). HIF- α is expressed in almost all cell types and directly or indirectly regulates the expression of more than 100 genes (9). The HIF-mediated hypoxia signaling pathway is involved in various biological processes, such as metabolism, angiogenesis, tumorigenesis, and immunity (10–14). Increased expression of HIF- α has been reported in the majority of tumor cell types and has been correlated with poor patient prognosis (15). HIF- α promotes tumor progression by regulating the expression of key target genes (16), as HIF-1 α supports tumor angiogenesis by enhancing the expression of vascular endothelial growth factor (*VEGF*) (17), and it also facilitates glucose uptake and glycolysis by upregulating the expression of glucose transporter 1 (*GLUT1*) and related genes (18).

Due to its canonical function in the hypoxia signaling pathway, *PHD2* is generally considered to be a tumor suppressor (3, 6). However, the effects of *PHD2* in tumorigenesis are not entirely dependent on HIF- α . The tumor-suppressing or tumor-promoting function of *PHD2* may depend on its different targets in different tumors (19, 20). In gastric cancer and prostate cancer, *PHD2* affects tumor development by inhibiting the HIF-mediated hypoxia signaling pathway (21–23). *PHD2* suppresses neoplastic growth in colon cancer and breast cancer by attenuating NF- κ B activity (24, 25). *PHD2* inhibits breast cancer growth by hydroxylating B55 α upon glucose starvation (26). *PHD2* regulates EGFR stability and subsequent signaling in breast cancer cells (27). *PHD2* acts in a hydroxylase-dependent manner to inhibit liver tumor cell proliferation and cyclin D1 expression (28). However, *PHD2* promotes cancer progression via hydroxylation of Carabin in B-cell lymphoma (29). Lung cancer ranks among the most common and dangerous malignancies. Based on histologic type, lung cancer can be divided into non-small cell lung cancer (NSCLC) and small cell lung cancer (SCLC), with NSCLC accounting for 80–85% of cases (30, 31). Based on the data obtained from the Cancer Genome Atlas (TCGA) database, we found that *PHD2* expression is upregulated in lung cancer, suggesting that *PHD2* may play a crucial role in lung cancer. However, the function of *PHD2* in NSCLC remains largely unknown.

In this study, we generated *PHD2*-deficient H1299 cells and *PHD2*-knockdown A549 cells to elucidate the function of *PHD2* in NSCLC, and found that *PHD2* suppressed cell proliferation and metabolism, but induced ROS levels in human NSCLC cells. The

function of *PHD2* in NSCLC is dependent on its enzymatic activity and partially independent of HIF. To further explore the mechanism of *PHD2* function in NSCLC, we performed RNA-seq and transcriptomic analysis, and identified some potential targets and pathways regulated by *PHD2*, apart from the canonical HIF-mediated hypoxia signaling pathway. These results provide some clues to discover novel roles of *PHD2* in lung cancer progression.

2 Materials and methods

2.1 Cell line and culture condition

H1299, A549 and HEK293T cells, initially obtained from the American Type Culture Collection (ATCC), were cultivated in Dulbeccos' modified Eagle medium (DMEM) (VivaCell Biosciences) supplemented with 10% fetal bovine serum (FBS) and maintained at 37°C in a humidified incubator containing 5% carbon dioxide (CO₂).

2.2 Generation of H1299 or A549 knockout/knockdown cell lines

For the generation of H1299 or A549 knockout/knockdown cell lines targeting the indicated genes, the sgRNA sequence was inserted into the Lenti-CRISPRv2 vector and then transfected into HEK293T cells together with viral packaging plasmids (psPAX2 and pMD2G). After transfection, the medium was changed 6 hours later, and the viral supernatant was harvested and filtered through a 0.45 μ m strainer. H1299 or A549 cells were then infected with viral supernatant and selected using 1 μ g/ml puromycin for 2 weeks. The sequence of the sgRNA targeting *PHD2* is: CCCGCCGCTGTC ATTGGCCA. The sequence of the sgRNA targeting *ARNT* is: GTCGCCGCTTAATAGCCCTC.

2.3 Generation of gene stably overexpressed cell lines

HEK293T cells were individually transfected with pHAGE empty, pHAGE-PHD2 or pHAGE-PHD2-H313A together with the packaging plasmids (psPAX2 and pMD2G). After 8 hours, the medium was removed and replaced with fresh medium containing 10% FBS, 10 μ M β -mercaptoethanol, and 1% streptomycin-penicillin. Forty hours later, the supernatants were harvested, filtered through a 0.45 μ m strainer, and subsequently applied to infect *PHD2*-deficient H1299 cells (*PHD2*^{-/-}) or *ARNT*-deficient H1299 cells (*ARNT*^{-/-}).

2.4 Western blot analysis and co-immunoprecipitation assay

Western blot analysis was performed as described previously (32). Antibodies comprising anti-PHD2 (#4835, Cell Signaling

Technology), anti-HIF1 α (#36169, Cell Signaling Technology), and anti-GAPDH antibody (#SC-47724, Santa Cruz Biotechnology) were used to detect the indicated proteins. The blots were photographed using a Fuji Film LAS4000 mini-luminescent image analyzer.

For the Co-immunoprecipitation assay, HEK293T cells were transfected with Myc-HIF-1 α together with Flag-PHD2 or Flag empty vector as a control. Immunoprecipitation was performed using anti-Flag antibody-conjugated agarose beads (#A2220, Sigma), and the interaction was analyzed by Western blot analysis with anti-Myc (#sc-40, Santa Cruz) and anti-Flag (#F1804, Sigma) antibodies.

2.5 Quantitative real-time PCR assay

RNAiso Plus (TaKaRa Bio., Beijing, China) was used for total RNA extraction according to the manufacturer's protocol. Revert Aid First Strand cDNA Synthesis Kit (Thermo Scientific, Waltham, MA, USA) was utilized for cDNA synthesis. MonAmp™ SYBR® Green qPCR Mix (high Rox) (Monad Bio., Shanghai, China) was employed for quantitative real-time PCR (qPCR) assays. The following primers were used: 5'-GATGCTAAAGCTATTTATGACT-3' and 5'-GGAATGACATCATTGTGTCGG-3' for *PDK1*; 5'-TGGCTTCTGGCATACTGCT-3' and 5'-GCTGCTTTCAGGACCACAGCT-3' for *PGK1*; 5'-TGTGGGCCTTTTCGTTAACC-3' and 5'-ATCATCAGCATTGAATTCCGC-3' for *GLUT1*; 5'-AGGAAGAACAGACCCCCAG-3' and 5'-CAGCACCACCCCAACAACACT-3' for *LDHA*; 5'-GAATTCCCAGTAAGTGGGG-3' and 5'-GGGCAGGGACTTAATCAACG-3' for *18SrRNA*.

2.6 Cell proliferation and colony formation assay

For the cell proliferation assay, H1299 cells were seeded in 96-well plates at a density of 1×10^3 cells per well and cultured for the indicated days. The CCK-8 assay was performed to assess cell growth rate following the manufacturer's instructions.

For the colony formation assay, H1299 cells were seeded in 6-well plates at a density of 1×10^3 cells per well and cultured for the indicated days. After seven days, colonies were fixed with methanol, stained with crystal violet (0.5% in methanol), rinsed with PBS, and then photographed. The colonies of appropriate size were individually counted from the images in each well.

2.7 Mitochondrial stress test and glycolytic rate test assays

The indicated H1299 cells (4×10^4 cells/well) were cultivated in XF24 cell culture microplate (#102340–100, Agilent Technologies). The XF Cell Mito Stress Test kit (#103015–100, Agilent Technologies) was used in the mitochondrial stress test assay to assess the oxygen consumption rate (OCR) using the Seahorse

XF24 Extracellular Flux Analyzer (Agilent Technologies, Santa Clara, CA, USA). The XF Glycolytic Rate Assay Kit (#103344–100, Agilent Technologies) was used in the glycolytic rate test assay to assess the proton efflux rate (PER) using the Seahorse XF24 Extracellular Flux Analyzer (Agilent Technologies, Santa Clara, CA, USA). Mitochondrial respiration, including basal respiration, maximal respiration, and spare respiratory capacity, were determined in the mitochondrial stress test assay by adding oligomycin (1.5 μ M), carbonyl cyanide-4-(trifluoromethoxy) phenylhydrazone (FCCP, 2 μ M), and antimycin A and rotenone mixture (0.5 μ M) to the cell culture plate. Glycolytic flux, including basal glycolysis and compensatory glycolysis, were determined in the glycolytic rate test assay by adding antimycin A and rotenone mixture (0.5 μ M) and 2-deoxy-D-glucose (50 mM) to the cell culture plate. Normalization to total cellular protein is used for the normalization of cells.

2.8 Glucose uptake assay

The fluorescent glucose analog 2-NBDG was used to evaluate glucose uptake. *PHD2*-deficient or wild-type H1299 cells (*PHD2*^{-/-} or *PHD2*^{+/+}) were grown in glucose-free DMEM medium for approximately 6 hours. After the addition of 50 μ M 2-NBDG, the cells were incubated in the dark at 37°C for 1 hour, and then the amount of 2-NBDG taken up by the cells was monitored by fluorescence microscopy or quantified by flow cytometry analysis (FACS).

2.9 Mitochondrial and intracellular ROS assay

MitoSOX™ Red (mitochondrial superoxide indicator) (#M36008, Thermo Fisher Scientific) and CM-H₂DCFDA (general oxidative stress indicator) (#C6827, Thermo Fisher Scientific) were used to determine mitochondrial and intracellular ROS levels, respectively. After cell harvest, cells were incubated with 5 μ M MitoSOX™ Red for 10 minutes at 37°C for the mitochondrial ROS assay, and with 1 μ M CM-H₂DCFDA for 1 hour at 37°C for the intracellular ROS assay.

2.10 RNA-Seq and bioinformatics analysis

Total RNA from *PHD2*-deficient or wild-type H1299 cells (*PHD2*^{-/-} or *PHD2*^{+/+}) was purified using the RNeasy Mini Kit (QIAGEN, 74104). Sequencing libraries were prepared using the NEBNext Ultra RNA Library Prep Kit for Illumina (NEB, USA, #E7530L) according to the manufacturer's protocol. Qualified libraries were pooled and sequenced on Illumina NovaSeq platforms using the PE150 strategy at Wuhan Benagen Technology Co., Ltd. (Wuhan, China). Fastp version 0.21.0 (<https://github.com/OpenGene/fastp>) was used to perform basic statistics on the quality of the raw reads. The clean reads were mapped to the human reference genome (hg38) using Star version 2.7.9a (<https://github.com/>

alexdbin/STAR). RSEM version 1.3.3 (<https://github.com/deweylab/RSEM>) was used to calculate gene and transcript expression levels expressed as fragments per kilobase of transcript per million fragments mapped (FPKM).

Gene expression levels in samples from *PHD2*-deficient H1299 cells were compared to those in samples from wild-type H1299 cells to identify differentially expressed genes (DEGs). DEGs were identified based on the following parameters: \log_2 (fold change) ≥ 1 and P value < 0.05 . The heatmap of the expression changes of the indicated genes and the volcano plot of the DEGs were generated using ImageGP (<https://www.bic.ac.cn/BIC/>). Gene Ontology (GO) enrichment analysis for the DEGs was performed using the clusterProfiler version 3.14.3 (<http://www.bioconductor.org/packages/release/bioc/html/clusterProfiler.html>). Kyoto Encyclopedia of Genes and Genomes (KEGG) enrichment analysis was performed using Gene Set Enrichment Analysis (GSEA) software (<http://software.broadinstitute.org/gsea/index.jsp>). The original RNA-seq data were uploaded to the GEO DataSets.

2.11 Immunofluorescence confocal microscopy

Cells were grown on glass coverslips overnight, and then fixed with 4% paraformaldehyde in PBS for 20 min, permeabilized with 0.1% Triton X-100, and blocked with 1% bovine serum albumin. Then, the cells were stained with anti-Ki67 primary antibody (#Ab16667, Abcam) followed by incubation with fluorescent-dye-conjugated secondary antibody. Nuclei were counterstained with DAPI (Sigma-Aldrich). Imaging of the cells was carried out using a Leica laser-scanning confocal microscope.

2.12 Statistical analysis

All statistical analyses were performed using GraphPad Prism software (8.3.0). Results with error bars represent mean \pm SD. Statistical analysis was based on Student's two-tailed t -test. A p -value less than 0.05 was regarded as significant. Statistical significance is presented as follows: * $p < 0.05$, ** $p < 0.01$, *** $p < 0.001$, **** $p < 0.0001$.

3 Results

3.1 *PHD2* deficiency enhances proliferation and metabolism in H1299 cells

Based on lung adenocarcinoma (LUAD) data extracted from the Cancer Genome Atlas (TCGA) database, we found that *PHD2* expression was higher in lung cancer tissues than in adjacent normal tissues (Figure 1A), indicating an essential role of *PHD2* in non-small cell lung cancer (NSCLC). Therefore, we knocked out *PHD2* in human NSCLC H1299 cells using CRISPR/Cas9 technology. Since *PHD2* interacts with HIF-1 α (Supplementary

Figure S1A), and *PHD2*-mediated hydroxylation leads to the degradation of HIF-1 α (Supplementary Figures S1B, C), the results of *PHD2* and HIF-1 α protein levels in Figure 1B indicated that *PHD2*-deficient H1299 cells were well established. In addition, increased mRNA levels of *PDK1*, *PGK1*, *GLUT1*, and *LDHA* indicated that *PHD2* was efficiently disrupted in *PHD2*-deficient H1299 cells (Figure 1C).

We then examined the effect of *PHD2* deficiency in H1299 cells. Proliferation of *PHD2*-deficient H1299 cells was faster than that of wild-type H1299 cells (Figure 1D), and the results were confirmed by immunofluorescence staining with anti-Ki67 antibody in H1299 cells (Supplementary Figure S2A). Similar results were obtained in human NSCLC A549 cells (Supplementary Figures S2B, C). Furthermore, *PHD2* deficiency resulted in increased basal glycolysis and compensatory glycolysis based on proton efflux rate (PER) measurement (Figures 1E, F), while spare respiratory capacity and maximal respiration of *PHD2*-deficient H1299 cells were significantly higher than that of wild-type H1299 cells based on mitochondrial stress test (Figures 1G, H). Furthermore, glucose uptake was strongly induced in *PHD2*-deficient H1299 cells (Figures 2A–C). In addition, we evaluated the effect of *PHD2* on the accumulation of reactive oxygen species (ROS) and found that mitochondrial ROS levels and intracellular ROS levels were significantly reduced in *PHD2*-deficient H1299 cells (Figures 2D–G). Taken together, these data suggest that *PHD2* deficiency promotes proliferation and metabolism in NSCLC cells.

3.2 *PHD2* function in NSCLC cells depends on its enzymatic activity

To assess whether the function of *PHD2* in NSCLC cells is dependent on its enzymatic activity, we reconstituted *PHD2* or its enzymatically deficient mutant (H313A) in *PHD2*-deficient H1299 cells by lentivirus. As expected, the spare respiratory capacity and maximal respiration of *PHD2*-deficient H1299 cells reconstituted with *PHD2* were lower than those of *PHD2*-deficient H1299 cells reconstituted with pHAGE empty vector, and the spare respiratory capacity and maximal respiration of *PHD2*-deficient H1299 cells reconstituted with *PHD2* were lower than those of *PHD2*-deficient H1299 cells reconstituted with *PHD2*-H313A mutant (Figures 3A, B). Similarly, mitochondrial ROS levels in *PHD2*-deficient H1299 cells reconstituted with *PHD2* were higher than those in *PHD2*-deficient H1299 cells reconstituted with pHAGE empty vector or *PHD2*-H313A mutant (Figures 3C, D). Similar results were obtained in the growth curve assay and the colony formation assay (Figures 3E–G). Taken together, these results suggest that *PHD2* function in NSCLC cells is dependent on its enzymatic activity.

3.3 Function of *PHD2* in NSCLC cells is at least partially independent of its canonical function in the hypoxia signaling pathway

PHD2-mediated hydroxylation and subsequent ubiquitination and degradation of HIF-1 α was considered to be the canonical and

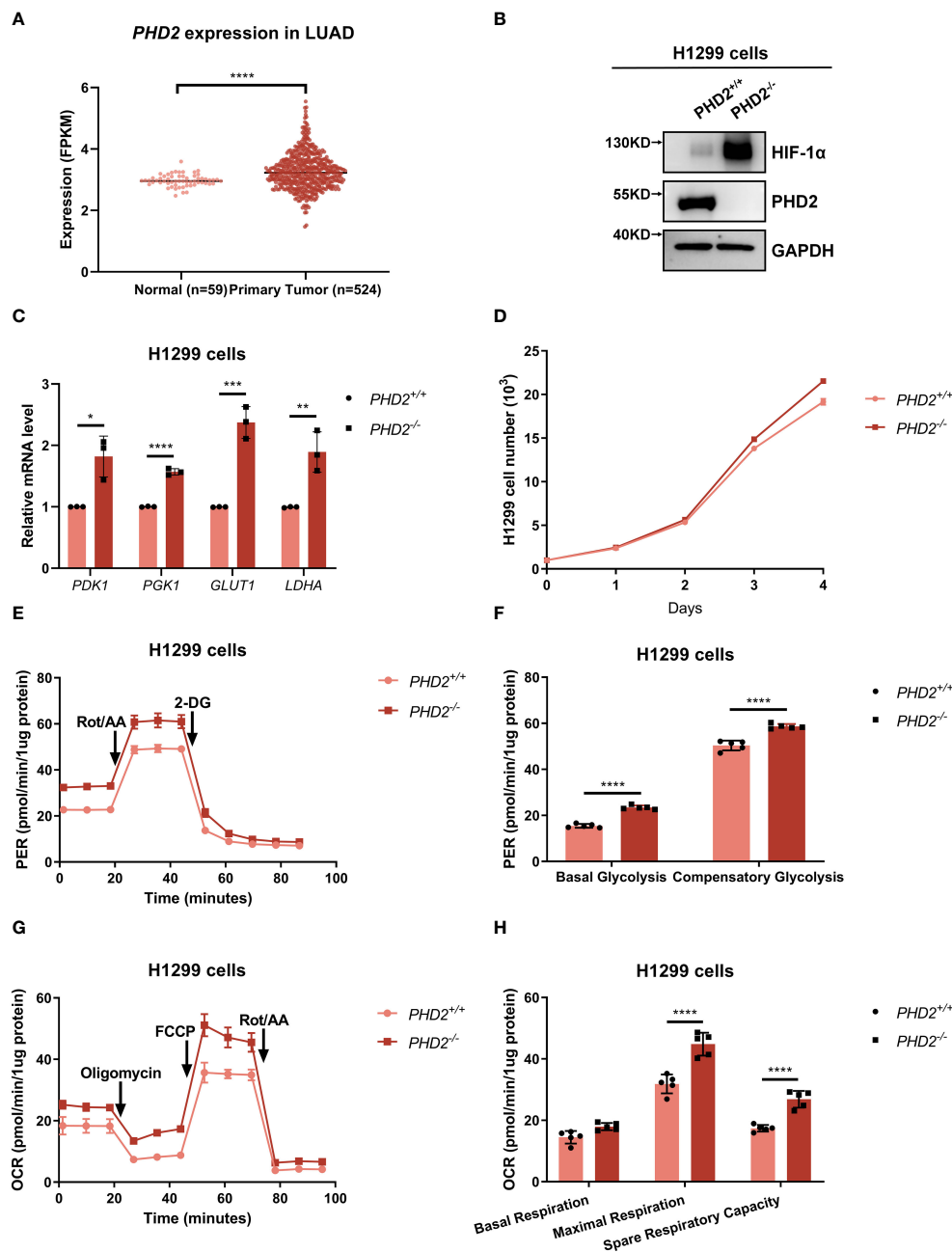


FIGURE 1

PHD2 deficiency enhances proliferation and metabolism in H1299 cells. (A) Expression data of *PHD2* in lung cancer tissues (n = 515) and adjacent normal tissues (n = 59) were obtained from The Cancer Genome Atlas (TCGA) data (<https://cancergenome.nih.gov/>). The mRNA levels of *PHD2* were higher in tumors than in normal tissues, as determined by Student's *t*-test; *****p* < 0.0001. (B) Western blot analysis of the indicated protein levels in *PHD2*-deficient or wild-type H1299 cells (*PHD2*^{-/-} or *PHD2*^{+/+}). (C) Quantitative real time PCR (qPCR) analysis of *PDK1*, *PGK1*, *GLUT1*, and *LDHA* mRNA in *PHD2*-deficient or wild-type H1299 cells (*PHD2*^{-/-} or *PHD2*^{+/+}). Data show mean ± SD; Student's two-tailed *t*-test; **p* < 0.05, ***p* < 0.01, ****p* < 0.001, *****p* < 0.0001; data from 3 independent experiments. (D) Growth curves of *PHD2*-deficient or wild-type H1299 cells (*PHD2*^{-/-} or *PHD2*^{+/+}) (n = 3) cultivated for the indicated days and analyzed by CCK-8 assay. (E, F) Changes in proton efflux rate (PER) in *PHD2*-deficient or wild-type H1299 cells (*PHD2*^{-/-} or *PHD2*^{+/+}) (n = 5) determined using the Seahorse XFe24 Extracellular Flux Analyzer. Statistics of compensatory glycolysis and basal glycolysis are shown in (F). (G, H) Changes in oxygen consumption rate (OCR) in *PHD2*-deficient or wild-type H1299 cells (*PHD2*^{-/-} or *PHD2*^{+/+}) (n = 5) determined using the Seahorse XFe24 Extracellular Flux Analyzer. Statistics of the capacity of maximal respiration, basal respiration, and spare respiratory are shown in (H).

most important function of *PHD2*, and the above results indicated that *PHD2* deficiency indeed led to the stabilization of HIF-1α and the induction of HIF target genes. Therefore, we investigated whether the function of *PHD2* in NSCLC cells is dependent on its canonical function in the hypoxia signaling pathway. We

generated *ARNT*-deficient H1299 cells and established *ARNT*-deficient H1299 cells reconstituted with *PHD2* or *PHD2*-H313A mutant by lentivirus. Stable overexpression with wild-type *PHD2* resulted in higher mitochondrial ROS levels than that with pHAGE empty vector or *PHD2*-H313A mutant (Figures 4A, B). In addition,

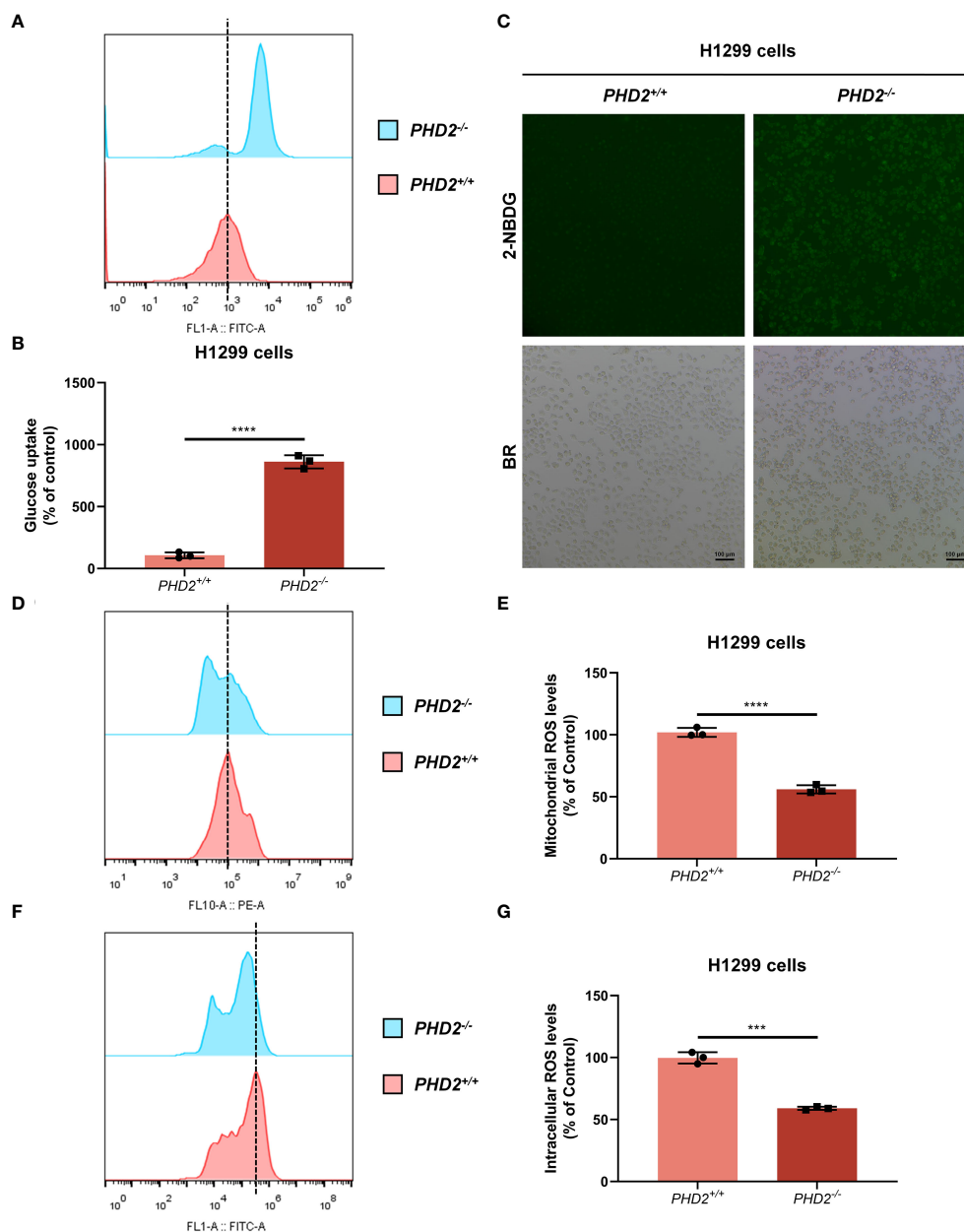


FIGURE 2

PHD2 deficiency promotes glucose uptake and reduces reactive oxygen species (ROS) levels in H1299 cells. (A–C) Glucose uptake in *PHD2*-deficient or wild-type H1299 cells (*PHD2*^{-/-} or *PHD2*^{+/+}) (*n* = 3) was analyzed using the fluorescent glucose analog 2-NBDG and evaluated by flow cytometry analysis (A, B) and fluorescence microscopy (C). (D, E) Mitochondrial ROS levels in *PHD2*-deficient or wild-type H1299 cells (*PHD2*^{-/-} or *PHD2*^{+/+}) were examined by flow cytometry analysis. Data represent mean ± SD; Student's two-tailed *t*-test; *****p* < 0.0001; data from 3 independent experiments. (F, G) Intracellular ROS levels in *PHD2*-deficient or wild-type H1299 cells (*PHD2*^{-/-} or *PHD2*^{+/+}) were examined by flow cytometry analysis. Data represent mean ± SD; Student's two-tailed *t*-test; ****p* < 0.001; data from 3 independent experiments.

the proliferation rate of *ARNT*-deficient H1299 cells stably overexpressed with empty vector or *PHD2*-H313A was higher than that of *ARNT*-deficient H1299 cells overexpressed with *PHD2*, as shown by growth curve assay and colony formation assay (Figures 4C–E). The trend in these *ARNT*-deficient H1299 cells was consistent with that in the *ARNT*-sufficient H1299 cells above. Therefore, these data suggest that *PHD2* function in NSCLC cells is at least partially independent of its canonical function in the hypoxia signaling pathway.

3.4 RNA-seq and transcriptomic analysis in *PHD2*-deficient or wild-type H1299 cells

Since the function of *PHD2* in NSCLC cells is partially independent of its canonical function in the hypoxia signaling pathway, we performed RNA-seq and transcriptomic analysis to explore the possible mechanisms of *PHD2* functions in lung cancer. The heatmap showed that the expression of HIF target genes, such as *MMP9*, *BNIP3*, *LDHA*, etc., was upregulated in *PHD2*-deficient

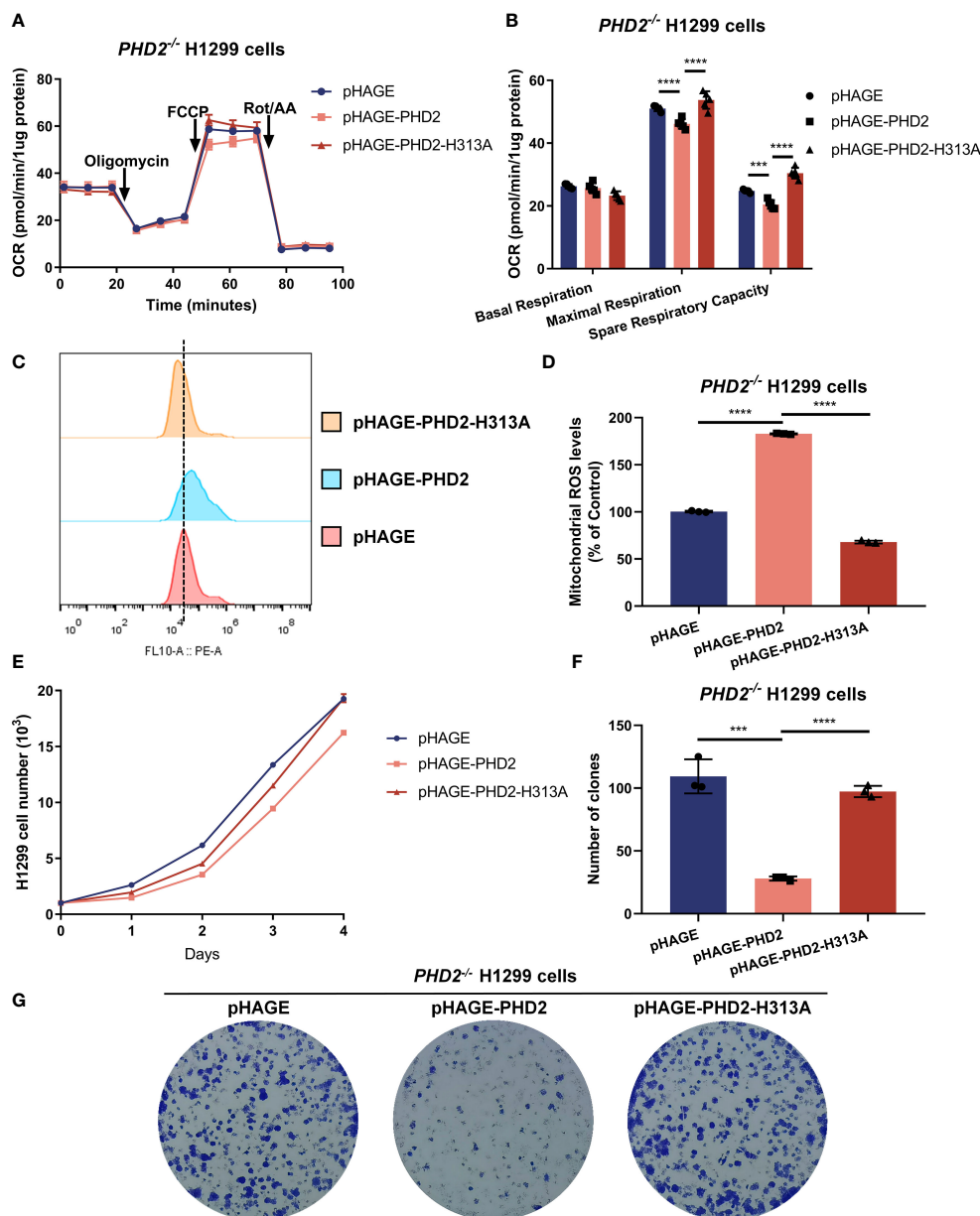


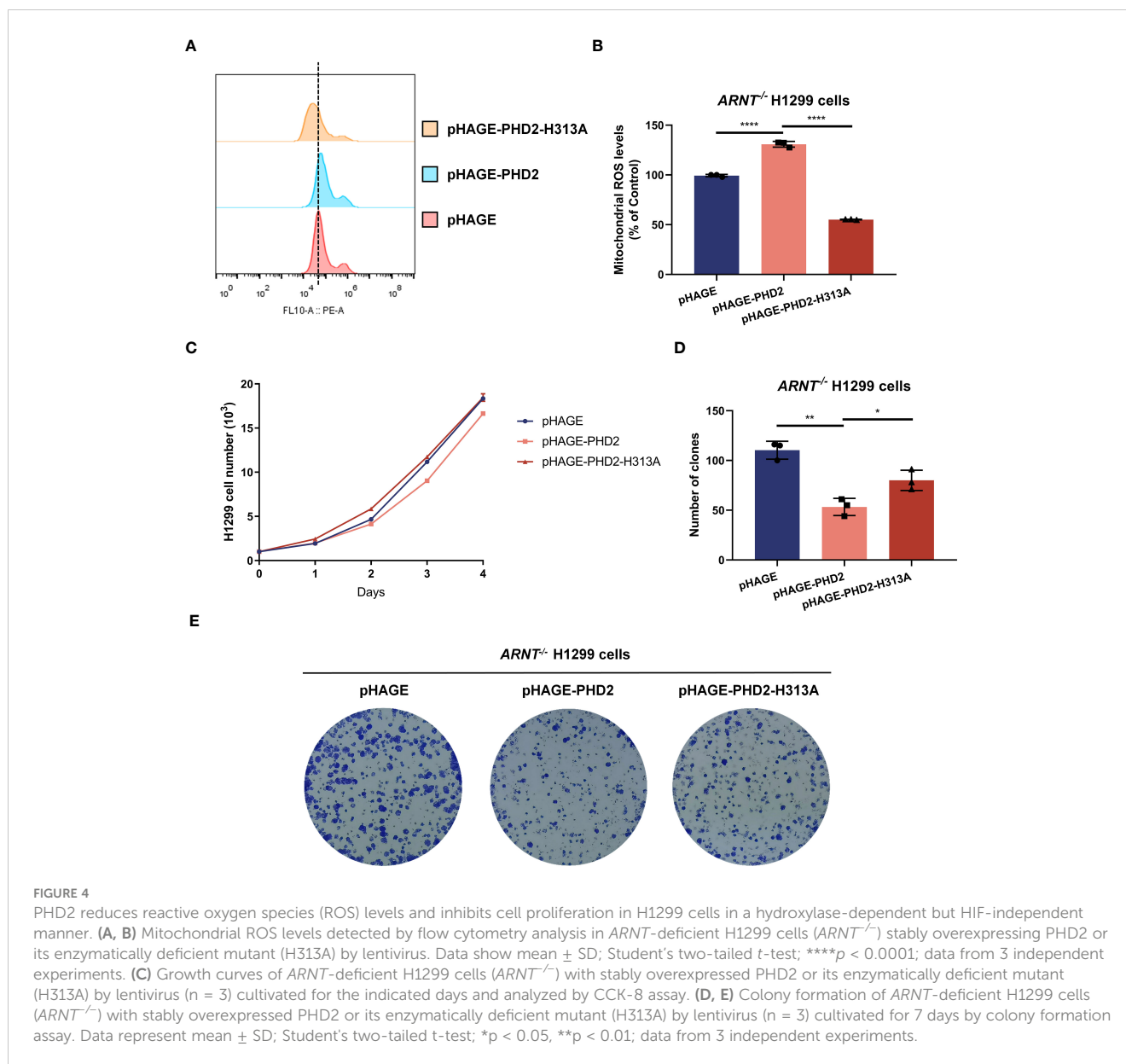
FIGURE 3

PHD2 impairs metabolism and proliferation in H1299 cells in a hydroxylase-dependent manner. (A, B) Seahorse XFe24 Extracellular Flux Analyzer was employed to assess the oxygen consumption rate (OCR) in *PHD2*-deficient H1299 cells (*PHD2*^{-/-}) reconstituted with PHD2 or its enzymatically deficient mutant (H313A) by lentivirus (n = 5). Statistics of maximal respiration, basal respiration, and spare respiratory capacity are shown in (B). (C, D) Mitochondrial ROS levels detected by flow cytometry analysis in *PHD2*-deficient H1299 cells (*PHD2*^{-/-}) reconstituted with PHD2 or its enzymatically deficient mutant (H313A) by lentivirus. Data represent mean ± SD; Student's two-tailed t-test; ***p < 0.001, ****p < 0.0001 data from 3 independent experiments. (E) Growth curves of *PHD2*-deficient H1299 cells (*PHD2*^{-/-}) reconstituted with PHD2 or its enzymatically deficient mutant (H313A) by lentivirus (n = 3), cultured for the indicated days and analyzed by CCK-8 assay. (F, G) Colony formation of *PHD2*-deficient H1299 cells (*PHD2*^{-/-}) reconstituted with PHD2 or its enzymatically deficient mutant (H313A) by lentivirus (n = 3), cultivated for 7 days, by colony formation assay. Data represent mean ± SD; Student's two-tailed t-test; ***p < 0.001, ****p < 0.0001; data from 3 independent experiments.

H1299 cells (Figure 5A). Moreover, the heatmap showed that the glycolysis/gluconeogenesis pathway-related genes were activated in *PHD2*-deficient H1299 cells (Figure 5B), and GSEA enrichment plots indicated that the glycolysis/gluconeogenesis pathway was significantly enriched in *PHD2*-deficient H1299 cells (Figure 5C). Some glycolysis/gluconeogenesis pathway-related genes overlapped with HIF target genes, such as *LDHA*, *PGK1*, *HK2*, etc., which may contribute to the fact that PHD2 can regulate the glycolysis pathway

through the HIF-mediated signaling pathway. In addition, the heatmap showed that the genes related to the oxidative phosphorylation pathway were also induced in *PHD2*-deficient H1299 cells (Figure 5D).

Gene Ontology (GO) analysis revealed that a number of biological processes, including extracellular matrix, cytoskeleton, metabolism, signal transduction, cell cycle, ion homeostasis, transcription, stem cell proliferation, etc., were enriched in *PHD2*-



deficient H1299 cells (Figure 6A). Among these processes, the cellular response to hypoxia pathway was indeed enriched, confirming the activation of the hypoxia signaling pathway in *PHD2*-deficient H1299 cells (Figure 6A). Furthermore, we found that some important signaling pathways related to tumor progression, including NF-kappaB (NF- κ B) signaling pathway, Notch signaling pathway, Wnt signaling pathway, and phosphatidylinositol 3-kinase (PI3K) signaling pathway, were enriched in *PHD2*-deficient H1299 cells (Figure 6B). Kyoto Encyclopedia of Genes and Genomes (KEGG) analysis revealed that several biological processes, including carbohydrate metabolism, amino acid metabolism, lipid metabolism, nitrogen metabolism, cell adhesion, gap junction, signal transduction, etc., were enriched in *PHD2*-deficient H1299 cells (Figure 7A). Similarly, we found that some important signaling pathways related to tumor progression, including PPAR signaling pathway, Hedgehog (Hh) signaling pathway, Calcium (Ca²⁺) signaling pathway, GnRH

signaling pathway, ErbB signaling pathway, and Wnt signaling pathway, were enriched in *PHD2*-deficient H1299 cell (Figure 7B). The volcano plot showed that some genes, such as *ITGB2* and *COL11A1*, were highly upregulated in *PHD2*-deficient H1299 cells, while other genes, such as *PRPF39* and *DTX3*, were highly downregulated in *PHD2*-deficient H1299 cells (Figure 7C). These results demonstrated that PHD2 likely has multiple targets in lung cancer, providing clues for understanding the potential mechanisms of PHD2 function in lung cancer progression.

4 Discussion

In this study, we analyzed the data obtained from the Cancer Genome Atlas (TCGA) database and observed that *PHD2* expression was higher in lung cancer tissues than in adjacent normal tissues. Similar findings have been reported by other

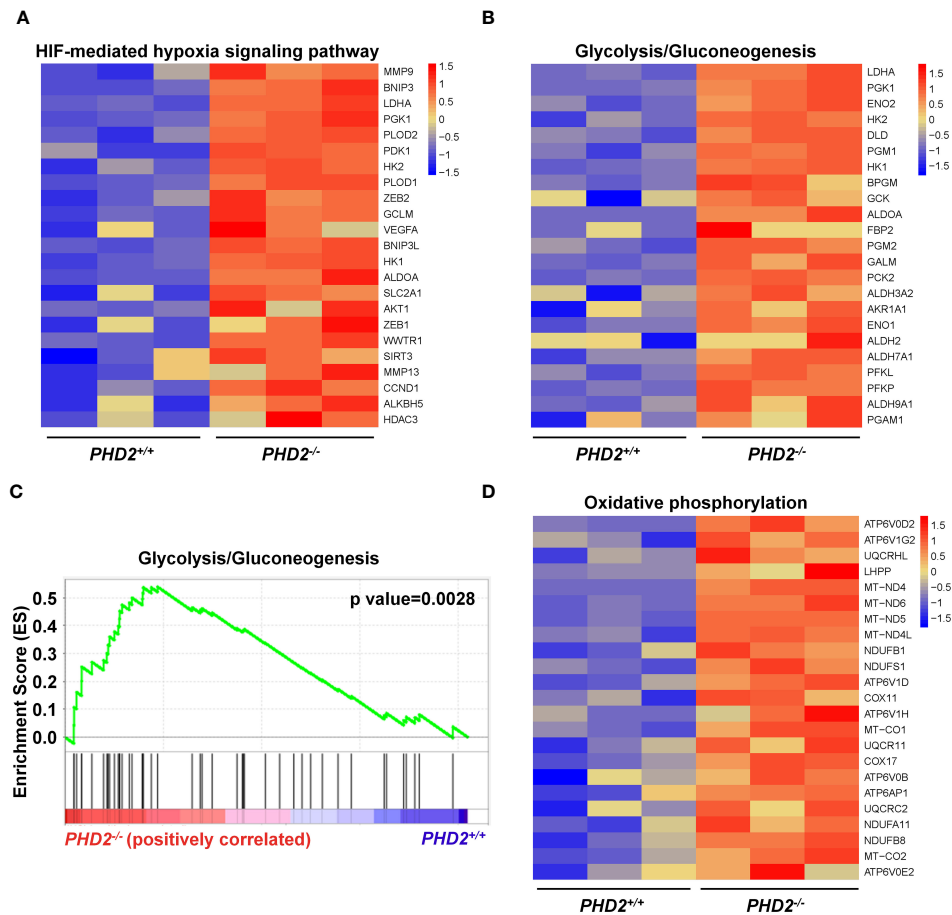


FIGURE 5

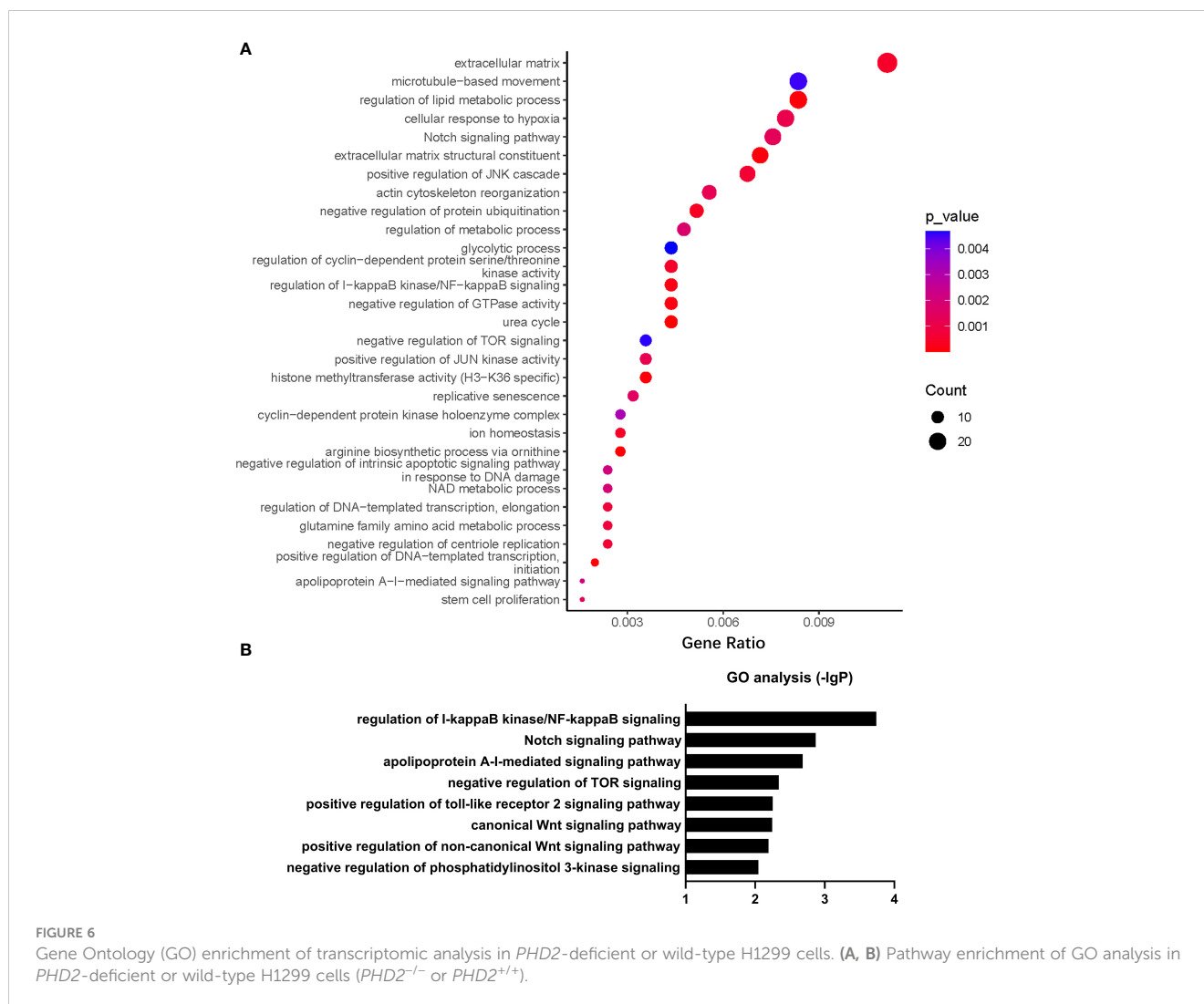
Enrichment of HIF target genes and metabolism-related genes in transcriptomic analysis in *PHD2*-deficient or wild-type H1299 cells. (A) Heatmap for expression of HIF target genes in *PHD2*-deficient or wild-type H1299 cells (*PHD2*^{-/-} or *PHD2*^{+/+}). (B) Heatmap for expression of genes related to the glycolysis/gluconeogenesis pathway in *PHD2*-deficient or wild-type H1299 cells (*PHD2*^{-/-} or *PHD2*^{+/+}). (C) GSEA enrichment plots of the glycolysis/gluconeogenesis pathway in *PHD2*-deficient or wild-type H1299 cells (*PHD2*^{-/-} or *PHD2*^{+/+}). Red represents high expression. Blue represents low expression. (D) Heatmap for expression of genes related to the oxidative phosphorylation pathway in *PHD2*-deficient or wild-type H1299 cells (*PHD2*^{-/-} or *PHD2*^{+/+}).

groups. Chen et al. investigated the mRNA levels of *PHD2* in 62 pairs of normal and NSCLC samples by RT-qPCR and found that *PHD2* expression was significantly higher in lung cancer tissues than in the adjacent normal tissues. Furthermore, *PHD2* expression was upregulated in 48 NSCLC patient samples (77.4% of the 62 samples) (33). However, Koren et al. investigated the expression of *PHD2* mRNA in 73 NSCLC primary tumors and 10 normal lung samples by RT-qPCR. The results showed that the expression of *PHD2* was significantly lower in lung cancer tissues than in normal tissues. Low expression of *PHD2* was associated with larger tumor size and worse prognosis in NSCLC patients (34). At present, there is no conclusion about the upregulation or downregulation of *PHD2* in lung cancer tissues. These different findings may be related to the variation in sample size or the discrepancy in tumor stage between different samples.

The enzymatic activity of PHD2 as a prolyl hydroxylase may deserve more attention than its expression level. Tumor cells generally proliferate rapidly and readily absorb oxygen and nutrients from blood vessels (35). However, as the tumor grows, the blood vessels become insufficient to supply the cells inside the

tumor. The cells inside the tumor are often in a hypoxic state. The lack of oxygen results in the inhibition of the enzymatic activity of PHD2, leading to the activation of the HIF-mediated hypoxia signaling pathway, which promotes tumor proliferation, migration and angiogenesis. Alteration of the enzymatic activity of PHD2 is an essential event during tumor progression, while the expression of PHD2 is likely to change subsequently with tumor development. In this study, we demonstrated that the suppressive effect of PHD2 on NSCLC is entirely dependent on its enzymatic activity, as enzymatic deficiency of PHD2 completely abolished the inhibition of PHD2 on tumor proliferation and metabolism, as well as the induction of ROS levels. Therefore, modulation of PHD2 enzymatic activity with specific inhibitors may play vital roles in the treatment of NSCLC.

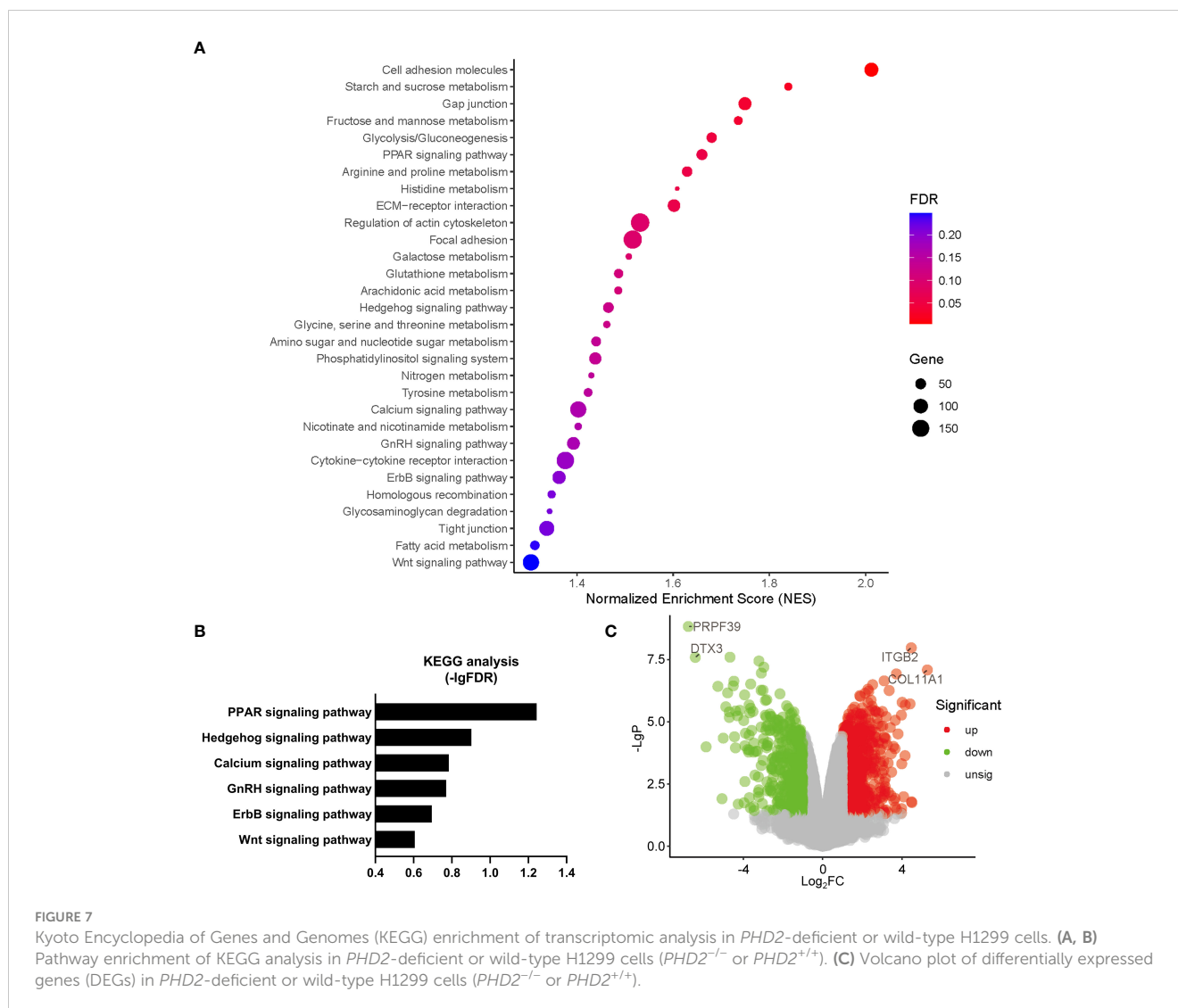
To explore the underlying mechanisms of PHD2 function in lung cancer progression, we performed RNA-seq and transcriptomic analysis in *PHD2*-deficient and wild-type H1299 cells. GO analysis showed that some important signaling pathways related to tumor progression, including NF- κ B signaling pathway, Notch signaling pathway, TOR signaling pathway, Wnt signaling pathway, and PI3K



signaling pathway, were enriched in *PHD2*-deficient H1299 cells. Meylan et al. showed that inhibition of the NF- κ B signaling pathway can significantly reduce tumor growth in lung cancer (36). PHD1 and PHD3 have been reported to negatively regulate the NF- κ B pathway through I κ B kinase β (IKK β) and heat shock protein 90 (Hsp90) (37–39). Takeda et al. showed that PHD2 negatively regulates NF- κ B activity in macrophages (40). In addition, both Notch1 and Notch3 have been reported to enhance cell proliferation and suppress apoptosis in NSCLC cells (41, 42). The LKB1/AMPK/mTOR signaling pathway has been identified as a tumor suppressor axis in NSCLC (43–45). Notably, inhibition of PHD has been reported to result in the inability of glutaminolysis to activate mTORC1 (46–48). These results suggest that PHD plays an aggressive role in the activation of mTORC1. Moreover, in this study, KEGG analysis revealed that some important signaling pathways related to tumor progression, including PPAR signaling pathway, Hh signaling pathway, Ca²⁺ signaling pathway, GnRH signaling pathway, ErbB signaling pathway, and Wnt signaling pathway, were enriched in *PHD2*-deficient H1299 cell. Similarly, abnormal activation of canonical and non-canonical Wnt signaling pathway has been observed in NSCLC in previous studies. Wen YA et al. reported

that silencing of *PHD2* rescued the expression of Wnt/ β -catenin pathway target genes in colon cancer (49). Similarly, the activation of the Hh signaling pathway was found to be enhanced in lung cancer. The Hh signaling pathway appears to play a critical role in promoting cell proliferation and angiogenesis (50, 51), while PHD2 inhibition can activate the Hh signaling pathway via the GPT2- α -KG-PHD2 axis in breast cancer (52). The volcano plot showed the most up- and down-regulated genes in *PHD2*-deficient H1299 cells, which may play an important role in lung cancer progression. These results suggest that PHD2 may have multiple targets and function through multiple pathways to fulfill its role in lung cancer progression. Further identification of the key targets of PHD2 in lung cancer progression will shed light on the treatment of NSCLC.

In this study, we have provided evidence that PHD2 suppresses cell proliferation and metabolism, but induces ROS levels in human NSCLC cells. Compared with the heterogeneity of tumor tissues, the homogeneity of NSCLC cell lines makes our results relatively stable and reliable. However, the actual function of PHD2 in NSCLC requires further verification using mouse models or a large number of patient samples. The function of PHD2 in NSCLC is dependent on its enzymatic activity and partially independent of HIF.



Transcriptomic analysis revealed some potential targets and pathways regulated by PHD2, providing some clues to discover some novel roles of PHD2 in lung cancer progression.

Data availability statement

The datasets presented in this study can be found in online repositories. The names of the repository/repositories and accession number(s) can be found below: <https://www.ncbi.nlm.nih.gov/geo/>, GSE239389.

Ethics statement

Ethical approval was not required for the studies on humans in accordance with the local legislation and institutional requirements because only commercially available established cell lines were used.

Author contributions

HD: Conceptualization, Data curation, Investigation, Methodology, Visualization, Writing – original draft. ZW: Investigation, Visualization, Writing – original draft. CZ: Investigation, Visualization, Writing – original draft. ZC: Conceptualization, Investigation, Methodology, Supervision, Writing – original draft, Writing – review & editing.

Funding

The author(s) declare financial support was received for the research, authorship, and/or publication of this article. This work was supported by Natural Science Foundation of Hubei Province of China (grant number ZRMS2017001052).

Acknowledgments

We are grateful to Fang Zhou for her help with fluorescence microscopy analysis and Yan Wang for her help with flow cytometry analysis. This work was supported by Natural Science Foundation of Hubei Province of China (grant number ZRMS2017001052).

Conflict of interest

The authors declare that the research was conducted in the absence of any commercial or financial relationships that could be construed as a potential conflict of interest.

References

- Bruick RK, McKnight SL. A conserved family of prolyl-4-hydroxylases that modify HIF. *Science*. (2001) 294:1337–40. doi: 10.1126/science.1066373
- Taylor MS. Characterization and comparative analysis of the EGLN gene family. *Gene*. (2001) 275:125–32. doi: 10.1016/S0378-1119(01)00633-3
- Jokilehto T, Jaakkola PM. The role of HIF prolyl hydroxylases in tumour growth. *J Cell Mol Med*. (2010) 14:758–70. doi: 10.1111/j.1582-4934.2010.01030.x
- Minervini G, Quaglia F, Tosatto SCE. Insights into the proline hydroxylase (PHD) family, molecular evolution and its impact on human health. *Biochimie*. (2015) 116:114–24. doi: 10.1016/j.biochi.2015.07.009
- Koivunen P, Tiainen P, Hyvarinen J, Williams KE, Sormunen R, Klaus SJ, et al. An endoplasmic reticulum transmembrane prolyl 4-hydroxylase is induced by hypoxia and acts on hypoxia-inducible factor alpha. *J Biol Chem*. (2007) 282:30544–52. doi: 10.1074/jbc.M704988200
- Fong GH, Takeda K. Role and regulation of prolyl hydroxylase domain proteins. *Cell Death Differ*. (2008) 15:635–41. doi: 10.1038/cdd.2008.10
- Kaelin WG, Ratcliffe PJ. Oxygen sensing by metazoans: The central role of the HIF hydroxylase pathway. *Mol Cell*. (2008) 30:393–402. doi: 10.1016/j.molcel.2008.04.009
- Wong BW, Kuchnio A, Bruning U, Carmeliet P. Emerging novel functions of the oxygen-sensing prolyl hydroxylase domain enzymes. *Trends Biochem Sci*. (2013) 38:3–11. doi: 10.1016/j.tibs.2012.10.004
- Weidemann A, Johnson RS. Biology of HIF-1 alpha. *Cell Death Differ*. (2008) 15:621–7. doi: 10.1038/cdd.2008.12
- Semenza GL. Oxygen sensing, hypoxia-inducible factors, and disease pathophysiology. *Annu Rev Pathol*. (2014) 9:47–71. doi: 10.1146/annurev-pathol-012513-104720
- Wheaton WW, Chandel NS. Hypoxia. 2. Hypoxia regulates cellular metabolism. *Am J Physiol-Cell Physiol*. (2011) 300:C385–93. doi: 10.1152/ajpcell.00485.2010
- Harris AL. Hypoxia - A key regulatory factor in tumour growth. *Nat Rev Cancer*. (2002) 2:38–47. doi: 10.1038/nrc704
- Corrado C, Fontana S. Hypoxia and HIF signaling: one axis with divergent effects. *Int J Mol Sci*. (2020) 21:17. doi: 10.3390/ijms21165611
- McGettrick AF, O'Neill LAJ. The role of HIF in immunity and inflammation. *Cell Metab*. (2020) 32:524–36. doi: 10.1016/j.cmet.2020.08.002
- Zhong H, De Marzo AM, Laughner E, Lim M, Hilton DA, Zagzag D, et al. Overexpression of hypoxia-inducible factor 1 alpha in common human cancers and their metastases. *Cancer Res*. (1999) 59:5830–5.
- Keith B, Johnson RS, Simon MC. HIF1 alpha and HIF2 alpha: sibling rivalry in hypoxic tumour growth and progression. *Nat Rev Cancer*. (2012) 12:9–22. doi: 10.1038/nrc3183
- Zagzag D, Zhong H, Scalzitti JM, Laughner E, Simons JW, Semenza GL. Expression of hypoxia-inducible factor 1 alpha in brain tumors - Association with angiogenesis, invasion, and progression. *Cancer*. (2000) 88:2606–18. doi: 10.1002/1097-0142(20000601)88:11<2606::AID-CNCR25>3.0.CO;2-W
- Chen C, Pore N, Behrooz A, Ismail-Beigi F, Maity A. Regulation of glut1 mRNA by hypoxia-inducible factor-1. Interaction between H-ras and hypoxia. *J Biol Chem*. (2001) 276:9519–25. doi: 10.1074/jbc.M010144200
- Li AQ, Zhang Y, Wang ZJ, Dong HL, Fu NG, Han XZ. The roles and signaling pathways of prolyl-4-hydroxylase 2 in the tumor microenvironment. *Chem-Biol Interact*. (2019) 303:40–9. doi: 10.1016/j.cbi.2019.02.019

Publisher's note

All claims expressed in this article are solely those of the authors and do not necessarily represent those of their affiliated organizations, or those of the publisher, the editors and the reviewers. Any product that may be evaluated in this article, or claim that may be made by its manufacturer, is not guaranteed or endorsed by the publisher.

Supplementary material

The Supplementary Material for this article can be found online at: <https://www.frontiersin.org/articles/10.3389/fonc.2024.1370393/full#supplementary-material>

- Strocchi S, Reggiani F, Gobbi G, Ciarrocchi A, Sancisi V. The multifaceted role of EGLN family prolyl hydroxylases in cancer: going beyond HIF regulation. *Oncogene*. (2022) 41:3665–79. doi: 10.1038/s41388-022-02378-8
- Lee SH, Bae SC, Kim KW, Lee YM. RUNX3 inhibits hypoxia-inducible factor-1 alpha protein stability by interacting with prolyl hydroxylases in gastric cancer cells. *Oncogene*. (2014) 33:1458–67. doi: 10.1038/onc.2013.76
- Guan D, Li CP, Li YL, Li YC, Wang GD, Gao FL, et al. The DpdtbA induced EMT inhibition in gastric cancer cell lines was through ferritinophagy-mediated activation of p53 and PHD2/hif-1 alpha pathway. *J Inorg Biochem*. (2021) 218:11. doi: 10.1016/j.jinorgbio.2021.111413
- Li Y, Zhang D, Wang XY, Yao X, Ye C, Zhang SJ, et al. Hypoxia-inducible miR-182 enhances HIF1 alpha signaling via targeting PHD2 and FIH1 in prostate cancer. *Sci Rep*. (2015) 5:13. doi: 10.1038/srep12495
- Bordoli MR, Stiehl DP, Borsig L, Kristiansen G, Hausladen S, Schraml P, et al. Prolyl-4-hydroxylase PHD2-and hypoxia-inducible factor 2-dependent regulation of amphiregulin contributes to breast tumorigenesis. *Oncogene*. (2011) 30:548–60. doi: 10.1038/onc.2010.433
- Wang L, Niu ZD, Wang X, Li ZX, Liu YY, Luo F, et al. PHD2 exerts anti-cancer and anti-inflammatory effects in colon cancer xenografts mice via attenuating NF-kappa B activity. *Life Sci*. (2020) 242:11. doi: 10.1016/j.lfs.2019.117167
- Di Conza G, Cafarello ST, Zheng XN, Zhang Q, Mazzone M. PHD2 Targeting Overcomes Breast Cancer Cell Death upon Glucose Starvation in a PP2A/B55 alpha-Mediated Manner. *Cell Rep*. (2017) 18:2836–44. doi: 10.1016/j.celrep.2017.02.081
- Kozlova N, Wottawa M, Katschinski DM, Kristiansen G, Kietzmann T. Hypoxia-inducible factor prolyl hydroxylase 2 (PHD2) is a direct regulator of epidermal growth factor receptor (EGFR) signaling in breast cancer. *Oncotarget*. (2017) 8:9885–98. doi: 10.18632/oncotarget.14241
- Tao YF, Lin F, Li RD, Shen J, Wang ZX. Prolyl hydroxylase-2 inhibits liver tumor cell proliferation and cyclin D1 expression in a hydroxylase-dependent manner. *Int J Biochem Cell Biol*. (2016) 77:129–40. doi: 10.1016/j.biocel.2016.05.022
- Jiang W, Zhou XY, Li ZX, Liu KY, Wang WG, Tan RK, et al. Prolyl 4-hydroxylase 2 promotes B-cell lymphoma progression via hydroxylation of Carabin. *Blood*. (2018) 131:1325–36. doi: 10.1182/blood-2017-07-794875
- Zappa C, Mousa SA. Non-small cell lung cancer: current treatment and future advances. *Transl Lung Cancer Res*. (2016) 5:288–300. doi: 10.21037/tlcr.2016.06.07
- Zheng M. Classification and pathology of lung cancer. *Surg Oncol Clin N Am*. (2016) 25:447. doi: 10.1016/j.soc.2016.02.003
- Tang J, Deng H, Wang Z, Zha H, Liao Q, Zhu C, et al. EGLN1 prolyl hydroxylation of hypoxia-induced transcription factor HIF1alpha is repressed by SET7-catalyzed lysine methylation. *J Biol Chem*. (2022) 298:101961. doi: 10.1016/j.jbc.2022.101961
- Chen SF, Zhang J, Li XB, Luo XY, Fang J, Chen HQ. The expression of prolyl hydroxylase domain enzymes are up-regulated and negatively correlated with Bcl-2 in non-small cell lung cancer. *Mol Cell Biochem*. (2011) 358:257–63. doi: 10.1007/s11010-011-0976-1
- Koren A, Rijavec M, Krumpstar T, Kern I, Sadikov A, Cufer T, et al. Gene expression levels of the prolyl hydroxylase domain proteins PHD1 and PHD2 but not PHD3 are decreased in primary tumours and correlate with poor prognosis of patients with surgically resected non-small-cell lung cancer. *Cancers*. (2021) 13:14. doi: 10.3390/cancers13102309

35. Lowry MC, O'Driscoll L. Can hi-jacking hypoxia inhibit extracellular vesicles in cancer? *Drug Discovery Today*. (2018) 23:1267–73. doi: 10.1016/j.drudis.2018.03.006
36. Meylan E, Dooley AL, Feldser DM, Shen L, Turk E, Ouyang C, et al. Requirement for NF-kappa B signalling in a mouse model of lung adenocarcinoma. *Nature*. (2009) 462:104–U115. doi: 10.1038/nature08462
37. Cummins EP, Berra E, Comerford KM, Ginouves A, Fitzgerald KT, Seeballuck F, et al. Prolyl hydroxylase-1 negatively regulates I kappa B kinase-beta, giving insight into hypoxia-induced NF kappa B activity. *Proc Natl Acad Sci U. S. A.* (2006) 103:18154–9. doi: 10.1073/pnas.0602235103
38. Fu J, Taubman MB. Prolyl hydroxylase EGLN3 regulates skeletal myoblast differentiation through an NF-kappa B-dependent pathway. *J Biol Chem*. (2010) 285:8927–35. doi: 10.1074/jbc.M109.078600
39. Xue J, Li XB, Jiao S, Wei Y, Wu GH, Fang J. Prolyl hydroxylase-3 is down-regulated in colorectal cancer cells and inhibits IKK beta independent of hydroxylase activity. *Gastroenterology*. (2010) 138:606–15. doi: 10.1053/j.gastro.2009.09.049
40. Takeda Y, Costa S, Delamarre E, Roncal C, de Oliveira RL, Squadrito ML, et al. Macrophage skewing by Phd2 haploinsufficiency prevents ischaemia by inducing arteriogenesis. *Nature*. (2011) 479:122–U153. doi: 10.1038/nature10507
41. Zou B, Zhou XL, Lai SQ, Liu JC. Notch signaling and non-small cell lung cancer (Review). *Oncol Lett*. (2018) 15:3415–21. doi: 10.3892/ol.2018.7738
42. Yuan X, Wu H, Han N, Xu HX, Chu Q, Yu SY, et al. Notch signaling and EMT in non-small cell lung cancer: biological significance and therapeutic application. *J Hematol Oncol*. (2014) 7:10. doi: 10.1186/s13045-014-0087-z
43. Shaw RJ, Cantley LC. Ras, PI(3)K and mTOR signalling controls tumour cell growth. *Nature*. (2006) 441:424–30. doi: 10.1038/nature04869
44. Ji HB, Ramsey MR, Hayes DN, Fan C, McNamara K, Kozlowski P, et al. LKB1 modulates lung cancer differentiation and metastasis. *Nature*. (2007) 448:807–U807. doi: 10.1038/nature06030
45. Han D, Li SJ, Zhu YT, Liu L, Li MX. LKB1/AMPK/mTOR signaling pathway in non-small-cell lung cancer. *Asian Pac. J Cancer Prev*. (2013) 14:4033–9. doi: 10.7314/APJCP.2013.14.7.4033
46. Duran RV, Oppliger W, Robitaille AM, Heiserich L, Skendaj R, Gottlieb E, et al. Glutaminolysis activates rag-mTORC1 signaling. *Mol Cell*. (2012) 47:349–58. doi: 10.1016/j.molcel.2012.05.043
47. Duran RV, MacKenzie ED, Boulahbel H, Frezza C, Heiserich L, Tardito S, et al. HIF-independent role of prolyl hydroxylases in the cellular response to amino acids. *Oncogene*. (2013) 32:4549–56. doi: 10.1038/onc.2012.465
48. Lorin S, Tol MJ, Bauvy C, Strijland A, Pous C, Verhoeven AJ, et al. Glutamate dehydrogenase contributes to leucine sensing in the regulation of autophagy. *Autophagy*. (2013) 9:850–60. doi: 10.4161/auto.24083
49. Wen YA, Xiong XP, Scott T, Li AT, Wang C, Weiss HL, et al. The mitochondrial retrograde signaling regulates Wnt signaling to promote tumorigenesis in colon cancer. *Cell Death Differ*. (2019) 26:1955–69. doi: 10.1038/s41418-018-0265-6
50. Velcheti V, Govindan R. Hedgehog signaling pathway and lung cancer. *J Thorac Oncol*. (2007) 2:7–10. doi: 10.1097/JTO.0b013e31802c0276
51. Abe Y, Tanaka N. The hedgehog signaling networks in lung cancer: the mechanisms and roles in tumor progression and implications for cancer therapy. *BioMed Res Int*. (2016) 2016:11. doi: 10.1155/2016/7969286
52. Cao Y, Lin SH, Wang YB, Chin YE, Kang L, Mi J. Glutamic pyruvate transaminase GPT2 promotes tumorigenesis of breast cancer cells by activating sonic hedgehog signaling. *Theranostics*. (2017) 7:3021–33. doi: 10.7150/thno.18992